Experimental Verification of the Very Strong Coupling Regime in a GaAs Quantum Well Microcavity

S. Brodbeck,[1] S. De Liberato,[2] M. Amthor,[1] M. Klaas,[1] M. Kamp,[1] L. Worschech,[1] C. Schneider,[1,*] and S. Höfling[1,3]

[1]Technische Physik, Physikalisches Institut and Wilhelm Conrad Röntgen-Research Center for Complex Material Systems, Universität Würzburg, Am Hubland, D-97074 Würzburg, Germany

[2]School of Physics and Astronomy, University of Southampton, Southampton SO17 1BJ, United Kingdom

[3]SUPA, School of Physics and Astronomy, University of St. Andrews, St. Andrews KY 16 9SS, United Kingdom

(Received 28 November 2016; published 12 July 2017)

The dipole coupling strength g between cavity photons and quantum well excitons determines the regime of light matter coupling in quantum well microcavities. In the strong coupling regime, a reversible energy transfer between exciton and cavity photon takes place, which leads to the formation of hybrid polaritonic resonances. If the coupling is further increased, a hybridization of different single exciton states emerges, which is referred to as the very strong coupling regime. In semiconductor quantum wells such a regime is predicted to manifest as a photon-mediated electron-hole coupling leading to different excitonic wave functions for the two polaritonic branches when the ratio of the coupling strength to exciton binding energy g/E_B approaches unity. Here, we verify experimentally the existence of this regime in magneto-optical measurements on a microcavity characterized by $g/E_B \approx 0.64$, showing that the average electron-hole separation of the upper polariton is significantly increased compared to the bare quantum well exciton Bohr radius. This yields a diamagnetic shift around 0 detuning that exceeds the shift of the lower polariton by 1 order of magnitude and the bare quantum well exciton diamagnetic shift by a factor of 2. The lower polariton exhibits a diamagnetic shift smaller than expected from the coupling of a rigid exciton to the cavity mode, which suggests more tightly bound electron-hole pairs than in the bare quantum well.

DOI: 10.1103/PhysRevLett.119.027401

Light-matter coupling in semiconductor microcavities can be categorized in different regimes, depending on the coupling strength g between cavity photons and quantum well excitons. In weak coupling, the presence of the microcavity modifies the radiative decay rate of the exciton [1]. For larger coupling strengths, a reversible energy transfer between excitons and photons takes place. This manifests in the appearance of two new eigenmodes in the strong coupling regime, the lower (LP) and upper polariton (UP), which are linear superpositions of the bare exciton and photon states. They are weighted by the Hopfield coefficients X and C which depend on g and detuning $\Delta = E_C - E_X$ between exciton (E_X) and photon energies (E_C) [2,3]. At zero detuning, LP and UP are separated by the Rabi splitting $\hbar\Omega \approx 2g$. As g becomes comparable to the exciton binding energy E_B, the light-matter coupling starts hybridizing different excitonic levels, effectively modifying the wave function of the electron-hole pair, in what has been named very strong coupling [4,5]. This leads to an additional, repulsive coupling term between electrons and holes for the UP, while electron-hole pairs are more tightly bound in the LP compared to the bare quantum well. Finally, if g is on the order of the exciton energy E_X, the coupling is intense enough to hybridize states with different numbers of excitations in the ultrastrong coupling regime [6–9].

In this Letter, we investigate an inorganic multiquantum well microcavity in a magnetic field revealing very strong coupling conditions. While in such inorganic quantum well microcavities for the exciton-photon coupling the condition $g \ll E_X$ holds, large ratios $\gamma = g/E_B > 0.5$ are regularly achieved [10–14]. Thus, while the hybridization of states with different numbers of excitations can be safely disregarded (rotating wave approximation), the mixing of different single-exciton states should play a non-negligible role. Still there has so far been no clear experimental confirmation of the modification of electron-hole coupling in the very strong coupling regime. To calculate the polariton states for large γ, a variational treatment has been developed [4,15,16], where the polariton wave function is a superposition of the photon state with an effective exciton wave function $\phi \propto \exp(-r_{eh}/\rho)/\rho$. Here, ρ is the average electron-hole separation $\rho = \langle (x_e - x_h)^2 + (y_e - y_h)^2 \rangle$, $x_{e,h}$ and $y_{e,h}$ are in-plane coordinates of the electron and hole, and $\langle\rangle$ denotes the expectation value. The ratio $\lambda = a_B/\rho$ is then used as a variational parameter to find the polariton energies. As a result, LP and UP are characterized by different ρ with $\rho_{\mathrm{LP}} < a_B$. ρ_{UP} can significantly exceed a_B due to photon-mediated mixing of the exciton ground state with continuum states as the UP lies close to the quantum well band gap for large γ. Both ρ_{LP} and ρ_{UP} are functions of Δ as well as γ. The strong

coupling regime at small γ, where the exciton is treated as a rigid harmonic oscillator [17], is recovered by setting $\rho_{\mathrm{LP}} = \rho_{\mathrm{UP}} = a_B$.

Recently, the diamagnetic shift of polaritons has been proposed as a method to verify the regime of very strong coupling [16] as the diamagnetic shift of an electron-hole pair is proportional to ρ^2 [18]. Applying an external magnetic field of strength B is a well-established tool for the investigation and manipulation of polaritons [19–21]. In the framework of strong coupling, the polariton energies are calculated from the Hamiltonian of two coupled oscillators [17]

$$H = \begin{pmatrix} E_X & g \\ g & E_C \end{pmatrix}. \tag{1}$$

With increasing magnetic field, the Rabi splitting increases [19,22–24] and the exciton energy exhibits a diamagnetic shift [18]

$$\delta E_X = \kappa_X B^2 = \frac{e^2}{8\mu}\rho^2 B^2, \tag{2}$$

where κ_X is the diamagnetic coefficient and μ the reduced mass of the quantum well exciton. The polariton energies as a function of magnetic field are then given by

$$E_{\mathrm{LP,UP}}(B) = \frac{E_X + E_C}{2} + \frac{1}{2}\left(\kappa_{\mathrm{LP,UP}}B^2 \mp \sqrt{[\hbar\Omega(B)]^2 + [\Delta - \kappa_{\mathrm{LP,UP}}B^2]^2}\right), \tag{3}$$

where we allow for $\rho_{\mathrm{LP}} \neq \rho_{\mathrm{UP}}$ considering different exciton diamagnetic coefficients for LP and UP and we account for a dependence of the Rabi frequency upon the applied magnetic field. While we do not have a theory describing the detailed interplay between very strong coupling and the applied magnetic field, we expect the former to be the dominant effect, allowing us to consider a lowest order approximation in B [15,21,25]. In the absence of a magnetic field, $\rho_{\mathrm{LP,UP}}$ in the very strong coupling regime can be calculated variationally as $\rho = a_B/\lambda$ with [4,15]

$$\lambda_\pm = 1 + \frac{\beta_\pm \gamma}{\alpha_\pm}, \tag{4}$$

where $\alpha_\pm^2 + \beta_\pm^2 = 1$ and

$$\alpha_\pm = \frac{1}{2} \pm \frac{\Delta/E_B - \gamma^2}{\sqrt{(\Delta/E_B - \gamma^2)^2 + 4\gamma^2}}. \tag{5}$$

We have measured the energies of LP and UP as a function of B for two different microcavity samples. In both samples, the cavity is formed by a $\lambda/2$-wide AlAs layer surrounded by $\mathrm{AlAs/Al_{0.2}Ga_{0.8}As}$ distributed Bragg reflectors with 16 (20) mirror pairs in the upper (lower) reflector. The low number of mirror pairs results in moderate Q factors around 1000 which allow for both polariton branches to be clearly resolved in reflectance for a wide range of detunings. Both samples were grown by molecular beam epitaxy on n-doped GaAs substrates. The first sample (1 QW sample) incorporates a single 7 nm wide GaAs quantum well in the center of the cavity. In the second sample (28 QW sample), a total number of 28 GaAs quantum wells with 7 nm width are placed in stacks of 4 quantum wells in the 7 central antinodes of the cavity light field [10]. AlAs barriers of 4 nm width separate the quantum wells. The maximum intensity of the antinodes decreases in the mirrors, which is why the quantum wells placed outside the cavity contribute less to the total coupling strength. While all quantum wells collectively couple to the same cavity mode, this inhomogeneity does not affect the resulting polariton wave functions that only depends on the superradiant coupling g.

The Rabi splittings of both samples are determined in radial reflectance measurements at 20 K where the spot of a white light source is scanned across the wafer. Because of the wedge shape of the cavity layer introduced during the epitaxial growth, the cavity mode is tuned through the exciton resonance in these measurements. Figures 1(a) and 1(b) show energies and linewidths of the polariton dips fitted to the reflectance spectra for the 1 QW sample and 28 QW sample, respectively [26]. For both samples, clear anticrossings of the cavity mode with the heavy hole exciton are observed. The Rabi splittings amount to

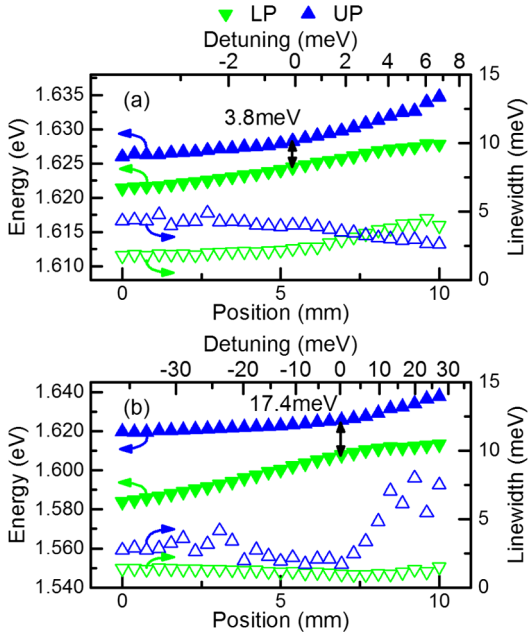

FIG. 1. Lower polariton (LP) and upper polariton (UP) energies (closed symbols) and linewidths (open symbols) as a function of sample position for samples with (a) 1 quantum well and (b) 28 quantum wells.

3.8 meV for the 1 QW sample and 17.4 meV for the 28 QW sample, close to the highest reported value for GaAs quantum wells of 19 meV for a similar sample design with 36 quantum wells [10]. With the exciton binding energy of 13.5 meV for a 7 nm wide GaAs quantum well in AlAs barriers [27], the ratios g/E_B are approximately 0.14 (0.64) for the 1 QW sample (28 QW sample). For the 28 QW sample, we observe a second anticrossing with the light hole exciton (not shown) that lies at an energy 30 meV above the heavy hole exciton. The cavity mode could not be tuned to this energy on the 1 QW sample. The Rabi splitting for the second anticrossing of the 28 QW sample amounts to 15.8 meV. The light hole-exciton fraction of the UP in Fig. 1(b) at zero detuning between cavity mode and heavy hole exciton is estimated to be below 0.05. This value has been determined from modeling the coupling of the cavity mode to both excitons as coupling of three harmonic oscillators, where the coupling term between the two excitons is zero [28]. We therefore neglect the influence of the light hole exciton in our study.

The polariton linewidths (full widths at half maximum) of the 1 QW sample, also plotted in Fig. 1(a), show the trend expected for strong coupling. In this regime, the polariton linewidth is the average of the photon and exciton linewidths that are weighted with the according Hopfield coefficients [2]. With increasing detuning the excitonic content of the LP (UP) increases (decreases). Since the exciton linewidth is larger than the photon linewidth in our samples, this results in a monotonically increasing (decreasing) linewidth for the LP (UP). Equal polariton linewidths are observed at slightly positive detuning, which may be a consequence of an asymmetric exciton linewidth [29]. For the 28 QW sample, a different behavior is observed as seen in Fig. 1(b). The LP linewidth is smaller than the UP linewidth for all detunings and reaches its smallest value (0.95 meV) at zero exciton-photon detuning. The UP linewidth also decreases towards zero detuning, but then shows a drastic increase for positive detunings, which is commonly observed in samples with large Rabi splittings and can be treated by including absorption by excited and continuum states in the quantum well dielectric function [10,14,30,31].

To confirm modifications of the average electron-hole separations predicted in the very strong coupling framework, we have measured diamagnetic shifts of the polariton branches in reflectance using a magnetocryostat where the samples are held at 5 K. Magnetic fields up to 5 T are applied along the growth direction (Faraday configuration). The samples are illuminated by a white light source and the signal is analyzed by imaging the Fourier plane of the objective onto a spectrometer. Polariton energies are determined by fitting line spectra at $k_{\parallel} = 0$ with Lorentzian functions. To measure the diamagnetic shift of the uncoupled heavy hole exciton, the upper mirrors of separate pieces of both wafers were removed by dry etching. The etched pieces are excited by a continuous wave Ti:sapphire laser with 3 mW power tuned to 1.72 eV and the photoluminescence is recorded. Linear least squares fits to the diamagnetic shifts as a function of B^2 yield diamagnetic coefficients of $\kappa_{X,1\ \mathrm{QW}} = (32.1 \pm 2.5)$ and $\kappa_{X,28\ \mathrm{QW}} = (36.7 \pm 2.8)\ \mu\mathrm{eV/T^2}$ for the two samples, comparable to values measured in similar samples [21,25]. The slightly smaller κ_X of the 1 QW sample indicates a narrower quantum well [18], in accordance with the slightly larger exciton energy of this sample; cf. Fig. 1.

Reflectance spectra at 0 and 5 T for the 1 QW sample at a detuning $\Delta = -3.4\ \mathrm{meV} = -0.89\ \hbar\Omega$ are shown in Fig. 2(a). Both polariton dips exhibit a blueshift with increasing magnetic field. It amounts to 118 μeV (714 μeV) for the LP (UP) at 5 T. Fitting the reflectance spectra with two Lorentzian functions yields the polariton energies as a function of magnetic field, which are plotted in Fig. 2(b). The polariton energies are fitted using Eq. (3) with $\kappa_{\mathrm{LP,UP}}$ as fitting parameters. Because of the small Rabi splitting of this sample and since an increase of only a few percent can be expected at 5 T [21,25], the contribution of an increase in Rabi splitting to the energy shifts is small; see also calculations of the net diamagnetic shift for various Rabi splitting increases in the Supplemental Material [26]. We have therefore assumed a constant Rabi splitting for the fitting procedure. The fits for both polaritons yield similar values for the diamagnetic coefficients of $\kappa_{\mathrm{LP}} = (30.1 \pm 1.4)$ and $\kappa_{\mathrm{UP}} = (32.1 \pm 0.9)\ \mu\mathrm{eV/T^2}$ in good agreement with $\kappa_{X,1\ \mathrm{QW}}$. This shows that the standard model for strong

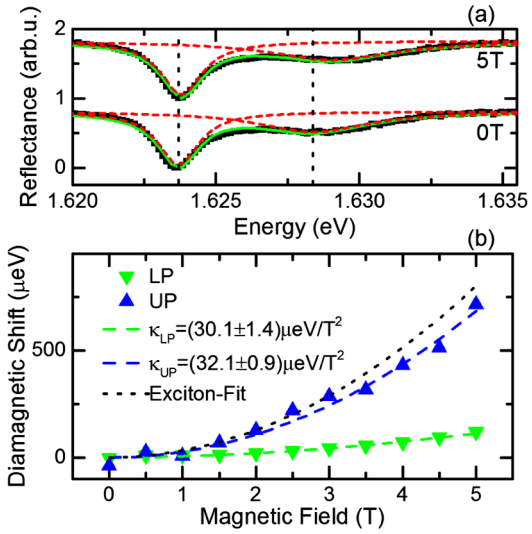

FIG. 2. (a) Reflectance spectra (black squares) at 0 and 5 T for the 1 QW sample at −3.4 meV detuning. The spectra are fitted with two Lorentzian functions (red dashed lines), green solid line shows the cumulative fit. Vertical dotted lines are the fitted polariton energies at zero magnetic field. (b) Diamagnetic shifts as a function of magnetic field. Dashed lines are fits according to Eq. (3) with κ as fitting parameter. Black dotted line is the fit to the bare exciton shift measured on a different piece of the same wafer.

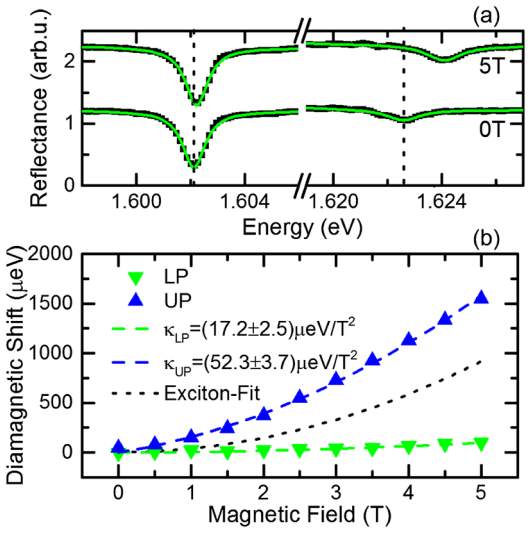

FIG. 3. (a) Reflectance spectra (black squares) at 0 and 5 T for the 28 QW sample at −10.8 meV detuning. Green solid line shows the fit with two Lorentzian functions. Vertical dotted lines are the fitted polariton energies at zero magnetic field. (b) Diamagnetic shifts as a function of magnetic field. Dashed lines are fits according to Eq. (3) with κ as fitting parameter. Black dotted line is the fit to the bare exciton shift measured on a different piece of the same wafer.

coupling that assumes rigid excitons can be applied for small γ.

The measurement of the diamagnetic shifts for the 28 QW sample at a detuning of $\Delta = -10.8$ meV $= -0.62\ \hbar\Omega$ is presented in Fig. 3. Figure 3(a) shows reflectance spectra at 0 and 5 T where again both polariton dips are shifted to higher energies with increasing magnetic field. At 5 T, the diamagnetic shift of the LP amounts to 98 μeV, while the shift of the UP amounts to 1.55 meV and significantly exceeds the bare exciton diamagnetic shift. For this sample, the increase of the Rabi splitting with increasing magnetic field gives a larger contribution to the polariton diamagnetic shift, but this alone cannot explain the observed shifts. If we assume a typical increase of 5% at 5 T as well as $\kappa_{\mathrm{LP}} = \kappa_{\mathrm{UP}} = \kappa_{X,28\ \mathrm{QW}}$, the expected diamagnetic shifts according to Eq. (3) are 1.07 meV for the UP and −153 μeV for the LP, which is negative in this calculation because the redshift due to an increasing Rabi splitting would exceed the blueshift due to the exciton diamagnetic shift. To fit the experimental data, we use Eq. (3) with $\hbar\Omega(B) = \hbar\Omega(0\mathrm{T}) + cB$ and treat κ and c as free parameters with the constraints $\kappa, c \geq 0$. Figure 3(b) depicts the diamagnetic shifts and fits as a function of magnetic field. For the LP, the best fit is achieved for $\kappa_{\mathrm{LP}} = (17.2 \pm 2.5)\ \mu\mathrm{eV/T}^2$, which is less than half as large as the bare exciton diamagnetic coefficient, and for constant Rabi splitting, i.e., $c = 0$. The fit to the UP diamagnetic shift on the other hand yields $\kappa_{\mathrm{UP}} = (52.3 \pm 3.7)\ \mu\mathrm{eV/T}^2$ and $c = (0.27 \pm 0.03)$ meV/T. The large differences in fitted values for κ and c for LP and UP indicate different electron-hole separations since both the diamagnetic shift of an exciton as well as the relative increase in oscillator strength are proportional to its radius at zero field [24].

The diamagnetic shifts of both polariton branches were measured at several different detunings for both microcavity samples. The total shifts at 5 T are summarized in Fig. 4(a) for the 1 QW sample and in Fig. 4(b) for the 28 QW sample. The LP exhibits similar shifts for both samples which increase with increasing detuning. For the UP on the other hand, there is a significant qualitative and quantitative difference between the two samples. For the 1 QW sample, the diamagnetic shift decreases with increasing detuning according to the decreasing excitonic content of the UP in the standard rigid exciton model. In stark contrast, the diamagnetic shift of the UP observed on the 28 QW sample increases with increasing detuning and exceeds the bare exciton shift in each measurement. With increasing detuning, the UP energy approaches the quantum well band gap energy which increases the contribution of continuum states. At a positive detuning of +1.9 meV, we measure a diamagnetic shift of 2.08 meV at 5 T for the UP, twice as large as the shift of the bare exciton and nearly 10 times as large as the shift of the LP for the same detuning (268 μeV). The fitted diamagnetic coefficients would yield an exciton radius of 7.2 nm (16.9 nm) for the LP (UP) [32] which visualizes the dominant contribution of higher resonances to the UP. The diamagnetic coefficient of the bare quantum well exciton $\kappa_{X,28\ \mathrm{QW}}$ corresponds to $a_B = 9.7$ nm.

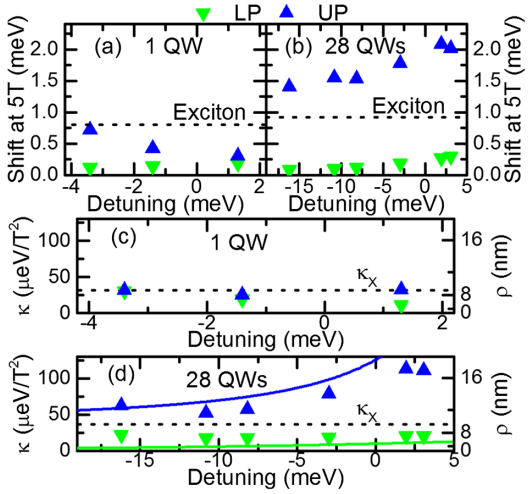

FIG. 4. Diamagnetic shifts of LP and UP at 5 T for (a) the 1 QW sample and (b) the 28 QW sample as a function of detuning. The shift of the UP of the 28 QW sample exceeds the bare exciton diamagnetic shift for all detunings. (c) Diamagnetic coefficients from fits according to Eq. (3) for the 1 QW sample. (d) The same as (c) for the 28 QW sample where κ_{UP} exceeds κ_X for all detunings. Solid lines are theoretical curves according to Eqs. (4) and (5), which yield $\rho_{\mathrm{LP,UP}}$ in the very strong coupling framework.

The diamagnetic shifts were all fitted with Eq. (3) with κ as fitting parameter. Figure 4(c) depicts the resulting diamagnetic coefficients for the 1 QW sample and Fig. 4(d) for the 28 QW sample. For the 1 QW sample, the Rabi splitting was assumed constant for all fits. κ_{LP} decreases with increasing detuning from 30.1 $\mu\mathrm{eV/T^2}$ at -3.4 meV down to 11.4 $\mu\mathrm{eV/T^2}$ at $+1.3$ meV. Because of the small Rabi splitting and moderate Q factor of this sample, the splitting between LP and UP in the considered detuning range barely exceeds the linewidths of the polaritons, which range from 2 to 4 meV. The LP linewidth increases with increasing detuning, Fig. 1(a), which could explain the unexpected decrease of κ_{LP} due to greater uncertainties in the fits of the reflectance spectra. The UP diamagnetic coefficient shows no clear trend with all values in the range of (30 ± 4) $\mu\mathrm{eV/T^2}$ close to the bare quantum well exciton diamagnetic coefficient of this sample. For the 28 QW sample, the polariton dips are well separated at all detunings due to the large Rabi splitting which facilitates fitting of the reflectance spectra. κ_{LP} is in the range of (19 ± 2) $\mu\mathrm{eV/T^2}$ for all detunings with no clear trend visible for increasing detuning. This value is roughly half as large as $\kappa_{X,28\ \mathrm{QW}}$. Additionally, the fitted values for c are below 8 $\mu\mathrm{eV/T}$ for all detunings, which also indicates a small ρ. κ_{UP} increases with increasing detuning and reaches values above 100 $\mu\mathrm{eV/T^2}$ for slightly positive detunings. The fitted values for c also show a slight increase with detuning with values in the range of (0.24 ± 0.10) meV/T. Both fit parameters are consistent with an increased ρ for the UP as predicted by the framework of very strong coupling. The diamagnetic coefficients for the 28 QW sample have also been calculated with the theoretical values for $\rho_{\mathrm{LP,UP}}$ according to Eqs. (4) and (5) which have no free parameters. The theoretical curves for very strong coupling are shown as solid lines in Fig. 4(d) and they are in good agreement with the values determined by fitting of the diamagnetic shifts with Eq. (3). Finally, we have calculated the net diamagnetic shift at 5 T for both samples in the coupled oscillator model using the measured values of κ_X, which are shown in the Supplemental Material [26]. For the 1 QW sample, there is good qualitative and quantitative agreement of theory and experiment which shows that treating LP and UP as linear combinations of photons with a rigid exciton is a good approximation for a small Rabi splitting. For the 28 QW sample on the other hand, the coupled oscillator model fails to reproduce the experimental values. It is essential to account for photon-mediated electron-hole coupling in this sample, e.g., by using polariton wave functions characterized by different ρ for LP and UP.

To conclude, we have shown that coupling to a cavity mode can modify not only the radiative decay of electron-hole pairs, but may also influence their formation mechanism. The very large diamagnetic shift of the UP that we measure for a sample with $g/E_B > 0.5$ is clear evidence of an increased average electron-hole separation due to photon-mediated mixing of the optically allowed interband transitions. For the LP, the comparably small diamagnetic shift indicates a reduced electron-hole separation which is explained in the framework of very strong coupling by increased electron-hole attraction due to photon-mediated interactions. This increased attraction could be exploited to realize polariton condensates at room temperature even in semiconductors like GaAs for which the exciton binding energy of a bare quantum well is smaller than the thermal energy at room temperature [15].

We thank M. Wagenbrenner and A. Wolf for assistance during sample preparation. Discussions with A. Schade and H. Suchomel are acknowledged. This work was supported by the State of Bavaria. S. D. L. acknowledges support from the Royal Society and from EPSRC Grant No. EP/M003183/1.

*christian.schneider@physik.uni-wuerzburg.de

[1] V. Savona, L. C. Andreani, P. Schwendimann, and A. Quattropani, Solid State Commun. **93**, 733 (1995).
[2] H. Deng, H. Haug, and Y. Yamamoto, Rev. Mod. Phys. **82**, 1489 (2010).
[3] J. J. Hopfield, Phys. Rev. **112**, 1555 (1958).
[4] J. B. Khurgin, Solid State Commun. **117**, 307 (2001).
[5] D. S. Citrin and J. B. Khurgin, Phys. Rev. B **68**, 205325 (2003).
[6] A. Vasanelli, Y. Todorov, and C. Sirtori, C.R. Phys. **17**, 861 (2016).
[7] C. R. Gubbin, S. A. Maier, and S. Kéna-Cohen, Appl. Phys. Lett. **104**, 233302 (2014).
[8] G. Scalari, C. Maissen, D. Turcinková, D. Hagenmüller, S. De Liberato, C. Ciuti, D. Schuh, C. Reichl, W. Wegscheider, M. Beck, and J. Faist, Science **335**, 1323 (2012).
[9] T. Niemczyk, F. Deppe, H. Huebl, E. P. Menzel, F. Hocke, M. J. Schwarz, J. J. Garcia-Ripoll, D. Zueco, T. Hümmer, E. Solano, A. Marx, and R. Gross, Nat. Phys. **6**, 772 (2010).
[10] J. Bloch, T. Freixanet, J. Y. Marzin, V. Thierry-Mieg, and R. Planel, Appl. Phys. Lett. **73**, 1694 (1998).
[11] H. Deng, G. Weihs, C. Santori, J. Bloch, and Y. Yamamoto, Science **298**, 199 (2002).
[12] J. Kasprzak, M. Richard, S. Kundermann, A. Baas, P. Jeambrun, J. M. J. Keeling, F. M. Marchetti, M. H. Szymanska, R. André, J. L. Staehli, V. Savona, P. B. Littlewood, B. Deveaud, and Le Si Dang, Nature (London) **443**, 409 (2006).
[13] G. Christmann, R. Butté, E. Feltin, J.-F. Carlin, and N. Grandjean, Appl. Phys. Lett. **93**, 051102 (2008).
[14] J.-R. Chen, T.-C. Lu, Y.-C. Wu, S.-C. Lin, W.-F. Hsieh, S.-C. Wang, and H. Deng, Opt. Express **19**, 4101 (2011).
[15] H. Zhang, N. Y. Kim, Y. Yamamoto, and N. Na, Phys. Rev. B **87**, 115303 (2013).
[16] M.-J. Yang, N. Y. Kim, Y. Yamamoto, and N. Na, New J. Phys. **17**, 023064 (2015).
[17] M. S. Skolnick, T. A. Fisher, and D. M. Whittaker, Semicond. Sci. Technol. **13**, 645 (1998).

[18] S. N. Walck and T. L. Reinecke, Phys. Rev. B **57**, 9088 (1998).
[19] J. D. Berger, O. Lyngnes, H. M. Gibbs, G. Khitrova, T. R. Nelson, E. K. Lindmark, A. V. Kavokin, M. A. Kaliteevski, and V. V. Zapasskii, Phys. Rev. B **54**, 1975 (1996).
[20] A. V. Larionov, V. D. Kulakovskii, S. Höfling, C. Schneider, L. Worschech, and A. Forchel, Phys. Rev. Lett. **105**, 256401 (2010).
[21] J. Fischer, S. Brodbeck, A. V. Chernenko, I. Lederer, A. Rahimi-Iman, M. Amthor, V. D. Kulakovskii, L. Worschech, M. Kamp, M. Durnev, C. Schneider, A. V. Kavokin, and S. Höfling, Phys. Rev. Lett. **112**, 093902 (2014).
[22] J. Tignon, R. Ferreira, J. Wainstain, C. Delalande, P. Voisin, M. Voos, R. Houdré, U. Oesterle, and R. P. Stanley, Phys. Rev. B **56**, 4068 (1997).
[23] B. Piętka, D. Zygmunt, M. Król, M. R. Molas, A. A. L. Nicolet, F. Morier-Genoud, J. Szczytko, J. Łusakowski, P. Zięba, I. Tralle, P. Stępnicki, M. Matuszewski, M. Potemski, and B. Deveaud, Phys. Rev. B **91**, 075309 (2015).
[24] P. Stępnicki, B. Piętka, F. Morier-Genoud, B. Deveaud, and M. Matuszewski, Phys. Rev. B **91**, 195302 (2015).
[25] J. Fischer, S. Brodbeck, B. Zhang, Z. Wang, L. Worschech, H. Deng, M. Kamp, C. Schneider, and S. Höfling, Appl. Phys. Lett. **104**, 091117 (2014).
[26] See Supplemental Material at http://link.aps.org/supplemental/10.1103/PhysRevLett.119.027401 for radial reflectance spectra at 0 T and a comparison of the measured net diamagnetic shift with a coupled oscillator model.
[27] L. C. Andreani and A. Pasquarello, Phys. Rev. B **42**, 8928 (1990).
[28] R. Balili, B. Nelsen, D. W. Snoke, L. Pfeiffer, and K. West, Phys. Rev. B **79**, 075319 (2009).
[29] A. V. Kavokin, Phys. Rev. B **57**, 3757 (1998).
[30] S. Faure, T. Guillet, P. Lefebvre, T. Bretagnon, and B. Gil, Phys. Rev. B **78**, 235323 (2008).
[31] S.-C. Lin, J.-R. Chen, and T.-C. LuAppl. Phys. B **103**, 137 (2011).
[32] M. Bayer, S. N. Walck, T. L. Reinecke, and A. Forchel, Phys. Rev. B **57**, 6584 (1998).